Alignment of ADS Beta Cryostat with Wire Position Monitor Postprint

Authors: ZHU Hong-Yan, DONG Lan, MEN Ling-Ling, LIU Can, LI Bo

Date: 2023-06-18T00:00:00+00:00

Abstract

Wire position monitor (WPM) is designed to monitor contraction of the cold masses during the cooling-down operation in an accelerator driven system. Because of material difference, machining error, assembly error, etc., each WPM has to be calibrated. The sensing voltage and wire position are of a nonlinear relationship, which is expressed by high order polynomial. Root mean square (RMS) of the polynomial fitting error were 3.8 m and 7.4 m at x and y directions, respectively. The alignment test was carried out on the beta cryostat. Optical instruments were used to verify the WPM measuring results. The differences between WPM measuring results and optical measurements were 0.044 and 0.05 mm in x and y direction, respectively. A significant asymmetric contraction was detected, and asymmetry of material was taken as the main reason through analysis.

Full Text

Preamble

Alignment of ADS Beta Cryostat with Wire Position Monitor

ZHU Hong-Yan (朱洪岩),† DONG Lan (董岚), MEN Ling-Ling (门瓴玲), LIU Can (刘璨), and LI Bo (李波)
Institute of High Energy Physics, Chinese Academy of Sciences, Beijing 100049, China

(Received August 25, 2014; accepted in revised form October 10, 2014; published online August 20, 2015)

Abstract: A wire position monitor (WPM) is designed to monitor contraction of cold masses during cool-down operations in an accelerator driven system. Due to material differences, machining errors, assembly errors, and other factors, each WPM must be calibrated. The relationship between sensing voltage

and wire position is nonlinear and can be expressed using high-order polynomials. The root mean square (RMS) of the polynomial fitting error was 3.8 µm and 7.4 µm in the x and y directions, respectively. Alignment tests were carried out on the beta cryostat, with optical instruments used to verify the WPM measurement results. The differences between WPM measurements and optical measurements were 0.044 mm and 0.05 mm in the x and y directions, respectively. A significant asymmetric contraction was detected, with material asymmetry identified as the primary cause through analysis.

Keywords: Wire position monitor, Alignment of cryostat, Wire position monitor calibration
DOI: 10.13538/j.1001-8042/nst.26.040401

Introduction

An accelerator driven system (ADS) is currently under development at the Institute of High Energy Physics (IHEP), Chinese Academy of Sciences. Most cavities and magnets operate within cryostats at liquid helium (LHe) temperature. Each cryostat contains six superconducting cavities and five superconducting magnets. Alignment is first performed at room temperature, and after thermal contraction, the positional error of the cavities and magnets must remain within ± 0.1 mm [**?**, **?**]. Conventional collimation methods are difficult to implement for measuring targets within the cryostat, and material contraction must be monitored throughout the thermal cycle. Therefore, a wire position monitor (WPM) was designed to track position changes caused by thermal contraction and expansion \cite{3–5}. The design and machining of the WPM have been completed [**?**].

Due to material differences, machining errors, assembly errors, and other factors, each WPM must be calibrated before use. A dedicated platform was designed for WPM calibration, followed by alignment experiments on the beta cryostat. Optical instruments were employed to verify the WPM measurement results.

II. Simulation

A. Calibration Simulation

Calibration simulation results obtained from CST Microwave Studio within a range of ± 4 mm in 0.5 mm steps are shown in Fig. 1

. The parameters Kx and Ky, defined as functions of wire position x and y, represent the sensitivity ratios:

$$Kx = x/U, \quad Ky = y/V$$

where U and V are the sensing voltages in the x and y directions, respectively. Kx and Ky remain approximately constant when x and y are small. However,

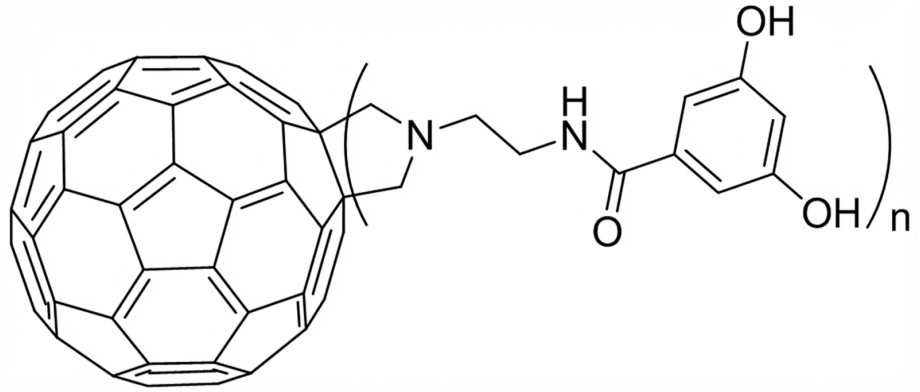

Figure 1: Figure 1

due to the probe geometry and microstrip angle, the relationship between sensing voltage and wire position in each direction is nonlinear. This relationship can be expressed using high-order polynomials [**?**, **?**]:

$$x = \sum_{i=0}^{k} \sum_{j=0}^{k-i} A_{ij} U^i V^j, \quad y = \sum_{i=0}^{k} \sum_{j=0}^{k-i} B_{ij} U^i V^j$$

where A and B are polynomial coefficients for each direction, and k is the polynomial order, which can be adjusted based on calibration results.

B. Influence of WPM Position Error

The inner radius of the WPM is 12 mm. The microstrips are 1 mm wide and 76 mm long, with their height calculated to achieve 50 Ω matching with the readout circuits [**?**]. The wire position monitor is supported within the cryostat by G10, a low thermal expansion coefficient insulation material. The setup is placed on a steel platform, with the connection structure between platform and WPM shown in Fig. 2(a) [FIGURE:2].

Due to assembly errors, the WPM may not be perfectly parallel with the wire. Four sets of simulations were conducted to analyze the influence of this position error. The coordinate system is aligned with the center of the WPM and the end of the microstrip (Fig. 2(b) [FIGURE:2]). Simulated position errors caused by wire tilting in 0.5° increments are presented in Table 1 , where L is the length of the strip and the coordinates represent rotation centers for each simulation.

TABLE 1. Position errors caused by wire tilt

Tilt angle (degree)	x = 0, y = 0, z = L/4	x = 0, y = 0, z = L/2	x = 0, y = 0, z = 0	x = 0, y = 2, z = L/2
0.5	-0.068	-0.145	-0.068	-0.145
1.0	-0.165	-0.318	-0.165	-0.318
1.5	-0.204	-0.403	-0.204	-0.403
2.0	-0.235	-0.572	-0.235	-0.572
2.5	-0.315	-0.656	-0.315	-0.656
3.0	-0.342	-0.782	-0.342	-0.782

The readout signal is a superposition of the upstream signal and the reflection from the downstream signal. The amplitudes of these two signals should be identical, and the readout signal effectively reflects the center position of the wire. Therefore, a position calculated from calibration simulation results is compared with the actual center position of the wire, with each value in Table 1 representing the error between them. The data show that the further the tilt center is from the WPM center, the larger the error becomes. When the tilt center is at the WPM center, the error can be ignored within $\pm 2^{\circ}$. However, the error cannot be ignored even within 0.5° when the tilt center changes.

An electronic level, optical level, and theodolite were used to adjust the relative position between the WPM probe and the wire. The electronic level was used to level the WPM probe, the optical level to level the wire, and the theodolite to adjust the parallelism of the vertical lines in the horizontal plane, which could be guaranteed within 10 .

III. Calibration Platform

A. Platform Structure

The WPM contains four Cu antennas supported by SMA jacks. The upstream ports connect to readout electronics to measure signal amplitude, while the downstream ports are terminated with 50 Ω loads. The monitor body is also made of Cu.

In the calibration platform (Fig. 3

), a fixed stretched wire serves as both a reference [**?**, **?**] and signal carrier, fed by a 215 MHz RF signal [**?**, **?**, **?**]. The WPM is attached to an electric translator stage with high position resolution up to 2 µm. The platform moves the WPM to simulate material contraction. The sensing signals from the four microstrip-antennas change with movement, and signal amplitude can be correlated to specific displacement after calibration [**?**, **?**].

B. Input and Termination Structure

The wire connections to the external RF signal and matching load are housed in two external boxes (Fig. 4 [FIGURE:4]). The input side is fixed, while the termi-

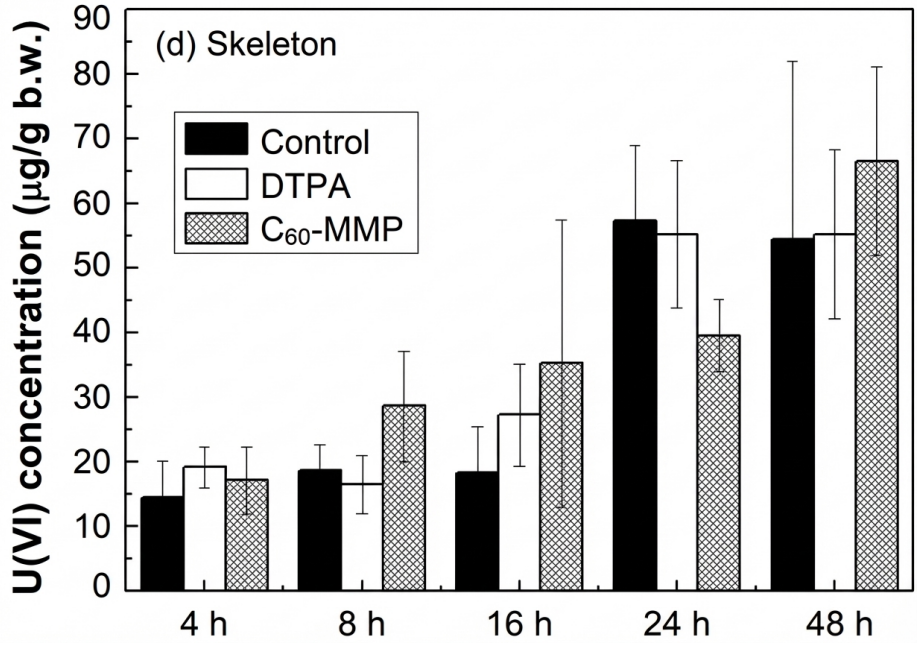

Figure 2: Figure 3

nation side is loaded with a set of steel blocks. At both ends, copper-beryllium wires are allowed to slide on G10 pulleys during contraction or expansion. The wire ends are clamped between G10 blocks, with the total weight of steel blocks being 5 kg [**?**].

C. Data Acquisition

Figure 5(a)

shows a diagram of the data processing circuits. A time-sharing system is employed, with digital I/O controlling RF switches for the WPMs [**?**]. Signals from the monitor are processed by a Bergoz card and transferred to a PC through a DAQ card to calculate wire position using calibrated coefficients. The sensing signals are shown in Fig. 5(b)

.

IV. WPM Calibration

The SMA jacks use PTFE insulation, which contracts as temperature decreases. This common-mode contraction in a symmetric structure is cancelled in differential circuits. Experimental results show that the reading difference between LN2 and room temperature is about 0.04 mm, partially caused by body contraction

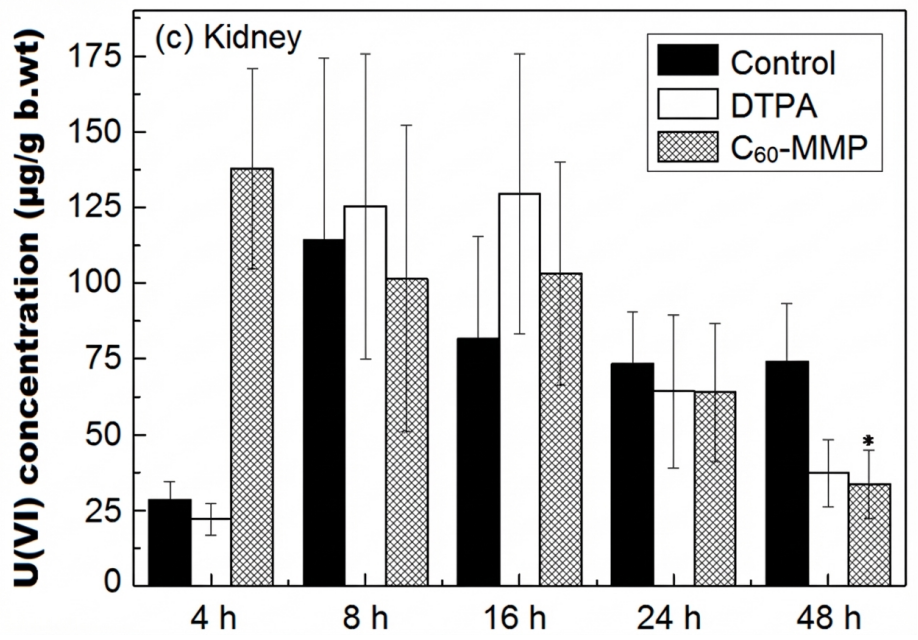

Figure 3: Figure 5

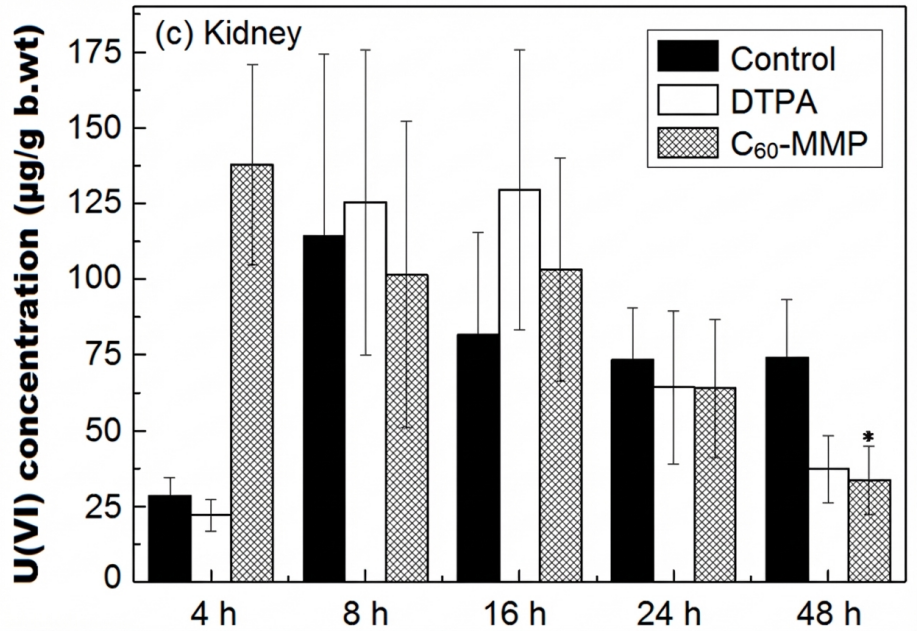

Figure 4: Figure 5

or temperature differential. Therefore, the wire position monitor is calibrated only at room temperature. Two calibration tests were performed: one within $r/2$ ($\pm$6 mm) in steps of 0.2 mm, and another within $r/3$ ($\pm$4 mm) in steps of 0.1 mm (Fig. 6 [FIGURE:6]). U–V represents the sensing voltage at each position, where 100 mV corresponds to 0.1 mm displacement at the center.

A sixth-order polynomial was used for the $r/2$ ($\pm$6 mm) mapping, and a fourth-order polynomial for the $r/3$ ($\pm$4 mm) mapping. The fitting results for the $r/3$ ($\pm$4 mm) mapping are given in Table 2 .

TABLE 2. The calibration coefficient (in mm) of $\pm$4 mm

Term	A (x-direction)	B (y-direction)
U^0V^0	-7.21×10^{-3}	-2.83×10^{-3}
U^0V^1	1.71×10^{-6}	-1.51×10^{-3}
U^0V^2	8.42×10^{-10}	2.22×10^{-10}
U^0V^3	1.60×10^{-13}	-3.93×10^{-11}
U^0V^4	1.58×10^{-16}	-1.11×10^{-16}
U^1V^0	-1.51×10^{-3}	-6.67×10^{-7}
U^1V^1	-2.21×10^{-10}	7.74×10^{-9}
U^1V^2	-3.79×10^{-11}	1.51×10^{-13}
U^1V^3	-8.58×10^{-18}	-2.00×10^{-16}
U^2V^0	-8.28×10^{-9}	-2.75×10^{-11}
U^2V^1	1.11×10^{-13}	-3.42×10^{-11}
U^2V^2	-1.33×10^{-16}	6.01×10^{-17}
U^3V^0	-3.20×10^{-11}	7.00×10^{-15}
U^3V^1	1.51×10^{-17}	9.24×10^{-16}
U^4V^0	1.33×10^{-15}	-9.51×10^{-17}

The coefficients A_{00} and B_{00} at U^0V^0 represent the offset between the geometric center and electrical center in each direction. The offset is -7.2 µm in the x-direction and -2.8 µm in the y-direction. A_{01} and B_{10} are first-order coefficients representing position resolution, where smaller values are better. The fitting results for $\pm$4 mm and $\pm$6 mm are consistent. The variances of fitting error are calculated as follows [**?**]:

$$S_{x-4mm} = \sqrt{\frac{\sum_{p=1}^{n}(x_{0p} - x_p)^2}{n}} = 3.8\,\mu m$$

$$S_{y-4mm} = \sqrt{\frac{\sum_{p=1}^{n}(y_{0p} - y_p)^2}{n}} = 7.4\,\mu m$$

$$S_{x-6mm} = 0.047\,mm, \quad S_{y-6mm} = 0.045\,mm$$

As shown in Fig. 7 [FIGURE:7], the fitting error for ±6 mm is much larger than that for ±4 mm.

V. Alignment Experiment

A. Experiment Setup

A complete thermal cycle was performed on the beta-cryostat, which was designed specifically for alignment testing. The beta-cryostat was 2 m long, with four WPMs symmetrically assembled beside a Φ1 m cavity made of 316 steel—the same material as its girder. A schematic layout of the WPMs and optical targets is shown in Fig. 8 [FIGURE:8]. The blue components are made of G10 material, which has low thermal conductivity and low thermal deformation [**?**], and is used as support for the WPMs, optical targets, and the bottom insulation layer.

When temperature decreases, the cavity and its girder contract. Attached to the cavity, a WPM experiences displacement in both horizontal and vertical directions [**?**, **?**]. The primary contraction of interest occurs between the cavity center and the girder bottom, with a distance of 0.419 m between them. Two optical targets placed at one end of the cryostat on the same support as the WPM experience the same displacement as the WPM. Levels were used to measure vertical displacement of the optical targets, while theodolites measured horizontal displacement. Optical measurements and WPM measurements were compared to verify accuracy.

B. Experiment Procedure

Beta-cryostat evacuation began at 8:00 on June 10, 2014, with vacuum reaching 0.1 Pa approximately 3 hours later. Figure 9 [FIGURE:9] shows horizontal and vertical displacements of the beta-cryostat during the entire thermal cycle. Optical measurements were time-consuming, so all measurements were taken during stable change periods. Figure 10 [FIGURE:10] shows the error between optical and WPM measurements.

The differences between WPM and optical measurements are within 0.1 mm, with variance of the difference being 0.044 mm in the x-direction and 0.05 mm in the y-direction. Considering alignment error and self-contraction of the optical target, the measurement results are consistent.

At the beginning, positive movement is observed in both vertical and horizontal directions as an effect of evacuation. The cool-down procedure began immediately after vacuum reached 0.1 Pa. Liquid N_2 was pumped into the Φ1 m cavity, causing a sharp displacement change. After slight recovery from this sudden change, contraction increased as temperature continued to decrease [**?**]. The figures reveal that contractions were not symmetrical, particularly in the x-direction. The maximum contraction difference was 0.4 mm in the x-direction

and 0.2 mm in the y-direction. This asymmetric contraction may cause facility center shift, making material symmetry a major design consideration [**?**, **?**].

Warm-up began at 12:00 on June 11, proceeding much slower than cool-down. Position was well recovered from both vertical and horizontal displacement after warm-up.

VI. Conclusion

Comparison results between optical measurements and WPM measurements demonstrate that WPM measurements are credible. Optical instrument usage requires personnel and only allows periodic readings. Conversely, WPM enables continuous monitoring, providing detailed contraction data valuable for characterizing new structures.

References

[1] Bosotti A, Pagani C and Varisco G. Online monitoring of the TTF cryostats cold mass with wire position monitors. INFN-LNF-TC–00-2, 2000.

[2] Bedeschi F, Bellettini G, Bosotti A, et al. A new wire position monitor readout system for ILC cryomodules. IEEE Nucl Sci Conf R, 2007, 1684–1686. DOI: 10.1109/NSS-MIC.2007.4437324

[3] Eddy N, Fellenz B, Prieto P, et al. A wire position monitor system for the 1.3 GHz tesla-style cryomodule at the fermilab New-Muon-Lab accelerator. 15th International Conference on RF Superconductivity(SRF2011), Chicago, Illinois, USA, Jul. 25–29, 2011. arxiv: 1209.4917

[4] Zhang D. A wire position monitor for superconducting cryomodules at fermilab. BIW'10, Santa Fe, NM, USA, May 2010, 187–188.

[5] Rawnsleyv W R, Giove D. ISAC-II cryomodule alignment monitor, TRIUMF Design Note, TRI-DN-03-02, 2003.

[6] Zhu H Y, Dong L and Li B. Design and simulation of a wire position monitor for cryogenic systems in an ADS linac. Chinese Phys C, 2014, 38: 087001. DOI: 10.1088/1674-1137/38/8/087001

[7] He X Y and Wu J. Calibration method of HLS's sensor used in SSRF. Nucl Sci Tech, 2008, 19: 321–324. DOI: 10.1016/S1001-8042(09)60011-7

[8] Ruan Y F. The study of the beam instruments for CSNS LINAC. Ph.D. Thesis, China Academy of Sciences, 2010. (in Chinese)

[9] Bowden G. Stretched wire mechanics. IWAA, TS08-3, CERN, Geneva, Switzerland, Oct. 2004.

[10] Wei M. Research on microstructure and mechanical properties of glass fiber/polyuria composites. Ph.D. Thesis, Harbin Institute of Technology, 2013. (in Chinese)

[11] Rawnsley W R. Alignment of the ISAC-II medium beta cryomodule with a wire monitoring system. 20th International Cryogenic Engineering Conference, Beijing, China, 2004.

[12] Bosotti A, Pagani C, Paparella R, et al. Mechanical vibration measurements on TTF cryomodules. IEEE Part Acc Conf, 2005, 434–436. DOI: 10.1109/PAC.2005.1590460

[13] Bosotti A. The wire position monitor(WPM) as a sensor for mechanical vibration for the TTF cryomodules. SRF'05, Cornell University, Ithaca, New York, USA, July 2005, 558–562.

[14] Stanford G, Bylinsky Y and Laxdal R E. Engineering and cryogenic testing of the ISAC-II medium beta cryomodule. Proceedings of LINAC 2004, Lübeck, Germany, 2004, 630–632.

[15] Deibele C. Matching BPM stripline electrodes to cables and electronics. Proceedings of 2005 Particle Accelerator Conference, Knoxville, Tennessee, 2005, 2607–2609.

[16] PCI1734 Digital IO Users' manual. Adcantech, Beijing, 2008.

[17] Shafer R E. Beam position monitor sensitivity for low-beta beams. AIP Conf Proc, 319: 303–308. DOI: 10.1063/1.46975

[18] Giove D, Bosotti A, Pagani C, et al. A wire position monitor (WPM) system to control the cold mass movements inside the TRF cryomodule. IEEE Part Acc Conf, 1997, 3: 3657–3659. DOI: 10.1109/PAC.1997.753375

[19] Forck P, Kowina P and Liakin D. Beam position monitor. Helmholtz Centre for Heavy Ion Research GSI. Germany,

[20] Suwada T, Kamikubota N, Fukuma H, et al. Stripline-type beam-position-monitor system for single-bunch electron/positron beams. Nucl Instrum Meth A, 2000, 440: 307–319. DOI: 10.1016/S0168-9002(99)00960-2

[21] Shintake T, Tejima M, Ishii H, et al. Sensitivity calculation of beam position monitor using boundary element method. Nucl Instrum Meth A, 1987, 254: 146–150. DOI: 10.1016/S0168-9002(87)90496-7